Available online at **www.joac.info**

ISSN: 2278-1862

Journal of Applicable Chemistry

2018, 7 (3): 608-615

(International Peer Reviewed Journal)

Thermal, Electrical and Structural Characteristics of $LiNi_{0.925}Mg_{0.075}PO_4$ and $LiNi_{0.9}Mg_{0.1}PO_4$ Cathode Materials

Paulos Taddesse[1]* and Mukemil Sultan[2]

1. Department of Physics, College of Natural Science, Arba Minch University, Arba Minch, **ETHIOPIA**
2. Grinzila Secondary School, Silte Zone, DalochaWereda, Dalocha, **ETHIOPIA**

Email:kidspaul@gmail.com

Accepted on 22nd April, 2018

ABSTRACT

Mg substituted lithium nickel phosphates, $LiNi_{0.925}Mg_{0.075}PO_4$ and $LiNi_{0.9}Mg_{0.1}PO_4$ cathode materials are synthesized by three steps solid state reaction method. These materials are characterized by thermogravimetric analysis (TGA), differential thermogravimetric analysis (DTA), x-ray powder diffraction (XRD), energy dispersive x-ray spectrometry (EDS), Fourier transform infrared (FT-IR) spectroscopy and complex impedance spectroscopy (CIS) techniques. From TGA/DTA study, compound formation temperature as well as the weight loss regions are identified. The XRD study of the prepared samples confirms the formation of good crystallization and well-defined diffraction peaks without impurities. From FT-IR study, different peaks are observed at different wavelength regions, which are responsible for the formation of both compounds. From the impedance analysis, it is found that the dielectric constant decreases sharply at low frequency as compared to that at high frequency and become almost constant on further increasing the frequency for both samples. The dc conductivity values of $LiNi_{0.925}Mg_{0.075}PO_4$ and $LiNi_{0.9}Mg_{0.1}PO_4$ are 3.8 x 10^{-9} Scm^{-1} and 3.94 x 10^{-9} Scm^{-1}, respectively. The obtained conductivity results are found in the range of the electrical conductivity of semiconductor (10^{-7} to 10^{3} Scm^{-1}), indicating the semiconductor behavior of the samples.

Graphical Abstract

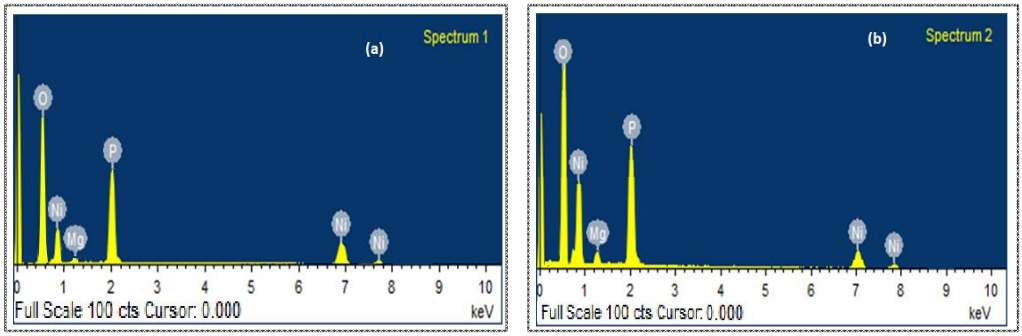

EDS spectra of (a) $LiNi_{0.925}Mg_{0.075}PO_4$ and (b) $LiNi_{0.9}Mg_{0.1}PO_4$ materials.

Keywords: Cathode materials, Solid state reaction method, Dielectric constant, Dc conductivity.

INTRODUCTION

In rechargeable lithium-ion batteries, cathode materials are one of the key components affecting the final performance of the batteries. New, unique and improved cathode materials are continuously developed. Among them, olivine structured lithium nickel phosphate ($LiNiPO_4$) cathode material has been recognized as one of the suitable cathode materials group for lithium ion batteries, due to its favorable characteristics such as long cycle life, good thermal stability, environment benignity and safety **[**1-3].

$LiNiPO_4$ cathode has an order olivine structure with space group Pmna in which Li and Ni ions occupy octahedral sites and P ions occupy tetrahedral sites [3, 4]. Also, Li and Ni ions occupy half of the octahedral sites and P ions occupy 1/8 of tetrahedral sites [4, 5].The oxygen ions in $LiNiPO_4$ crystal form strong covalent bonds with Phosphorous ions (P^{5+}) to form the PO_4 tetrahedral polyanion and stabilize the entire three-dimensional frameworks which provide improved stability and extreme safety under abusive conditions [6, 7]. This means that they do not experience the capacity fade during cycling suffered by lithium transition metal oxides such as $LiCoO_2$, $LiNiO_2$ $LiMn_2O_4$ and $LiMnO_2$ [2].

In the crystal structure of $LiNiPO_4$, NiO_6 is a corner shared octahedron and PO_4 is an edge shared tetrahedron, and they form the zigzag skeleton by sharing oxygen [5, 7]. Such framework structures containing an interconnected interstitial space are potentially fast ionic conductors, especially if the substitution of the larger polyanion in an open 3D lattice helps stabilizing the structure and the 3D tunnel network allowing for fast ion migration. Further, all the PO_4 tetrahedral of $LiNiPO_4$ don't touch each other. However, the corner shared NiO_6 octahedral of $LiNiPO_4$ which are separated by the oxygen atoms of the PO_4 tetrahedral cannot form a continuous NiO_6 network, which results in the poor electronic conductivity of $LiNiPO_4$ [1, 8].

$LiNiPO_4$ cathode material has attracted the wonderful attention of researchers due to its high energy density, low raw material cost, low toxic as well as environmentally friendly nature, good thermal stability at fully charged state, very stable during charge/discharge process, and high safety [3, 9]. However, the drawback of this material is its very low electronic conductivity [9, 10], as discussed above. For instance, the room temperature electronic conductivity of $LiNiPO_4$ is about 10^{-14} S cm^{-1}, being much lower than that of $LiCoO_2$ (~10^{-3} S cm^{-1}) and $LiMn_2O_4$ (2×10^{-5}- 5×10^{-5} S cm^{-1}) [3, 5]. Different experimental approaches have been proposed to solve the problems, including partial substitution of Ni by other metal elements, like Mn, Co, Fe, etc., coating with conductive substance such as Ag, Cu, conductive carbon, during the synthesis process reduction of grain size so as to shorten the Li-ion diffusion length and synthesis of particles with well-defined morphology [5, 8].

In this study, Mg^{2+} substituted $LiNi_{0.925}Mg_{0.075}PO_4$ and $LiNi_{0.9}Mg_{0.1}PO_4$ olivine structured cathode materials are synthesized by three steps solid reaction method. Phase purity for these two cathode materials is confirmed by XRD. Different structural parameters are also calculated from XRD data. The existence of all elements in both cathode materials is identified by EDS. The decomposition route and cathode formation are investing using TGA/DTA technique. The prepared cathodes are also characterized using FT-IR spectroscopy to confirm the formation of both compounds. In addition, the electrical as well as the dielectric properties studies of both compounds are discussed in comparison with $LiNiPO_4$.

MATERIALS AND METHODS

Powder Preparation: $LiNi_{0.925}Mg_{0.075}PO_4$ and $LiNi_{0.9}Mg_{0.1}PO_4$ powder samples are synthesized by three steps solid state reaction method using $LiNO_3$, $Ni(NO_3)_2.6H_2O$, MgO and $NH_4H_2PO_4$ raw materials. A stoichiometric amount of these raw materials is heated together at a temperature of 300°C for 3 h in air furnace to dry the mixture. The obtained powder materials are grounded again for

about 2 h, and then heated at 500°C for 3 h in air to make the samples free from gases. The obtained powder again grounded for one hour. Further, the final powder materials are calcined at 700°C for 8 h under flowing argon gas with a heating and cooling rate of 5°C min^{-1} to obtain single phase $LiNi_{0.925}Mg_{0.075}PO_4$ and $LiNi_{0.9}Mg_{0.1}PO_4$ materials. After cooling the mixture to room temperature, they are grounded for about 30 mins in an agate mortar to obtain fine powder materials.

Characterization Techniques: the simultaneous TGA/DTG analysis is conducted using PL-STA 1500 instrument in oxygen atmosphere by heating the precursors from room temperature to 850°C at a heating and cooling rate of 10°C min^{-1}. The crystal structure of both powder samples is characterized by XRD at room temperature by Philips APD 3720 X-ray diffractometer with Cu Kα radiation of wavelength λ = 1.54178 Å at a diffraction angle between 2θ = 15° and 45°. FT-IR spectroscopy measurements are accomplished by Shimadzu FT-IR-8900 instrument in transmittance method with potassium Bromide (KBr) as IR window in the wave number region of 400 to 1,200 cm^{-1}. The electrical and dielectric properties of electrodes are performed by Phase Sensitive Multimeter (Model: PSM 1700, UK).

RESULTS AND DISCUSSION

Thermal analysis: The TGA and DTA curves, for the thermal decomposition of the mixture of the precursors measured at a heating rate of 10°C min^{-1} in flowing oxygen is shown in figure 1. As observed from both curves, there is an initial weight loss in the temperature range from room temperature to 250°C, which corresponds to the evaporation of methanol we used during grinding to homogenize the mixture and the moisture absorbed during storage. For $LiNi_{0.925}Mg_{0.075}PO_4$ compound, significant weight loss about 27 wt% is observed between the temperatures 400 and 540°C. This loss is attributed to the decomposition of the precursors $LiNO_3$, $Ni(NO_3)_2.6H_2O$, MgO and $NH_4H_2PO_4$. This effect is supported by sharp exothermic peak observed at about 441.6°C on the DTG curve. At higher temperatures, the TGA curve becomes more flattened, indicating the stable phase formation of crystalline $LiNi_{0.925}Mg_{0.075}PO_4$.

For $LiNi_{0.9}Mg_{0.1}PO_4$ compound, significant weight loss about 30 wt% is observed between the temperatures 400 and 550°C. This loss is attributed to the decomposition of the precursors $LiNO_3$, $Ni(NO_3)_2$. $6H_2O$, MgO and $NH_4H_2PO_4$.This effect is supported by sharp exothermic peak observed at about 446°C on the DTG curve. At higher temperatures, the TGA curve becomes more flattened, indicating the stable phase formation of $LiNi_{0.9}Mg_{0.1}PO_4$.

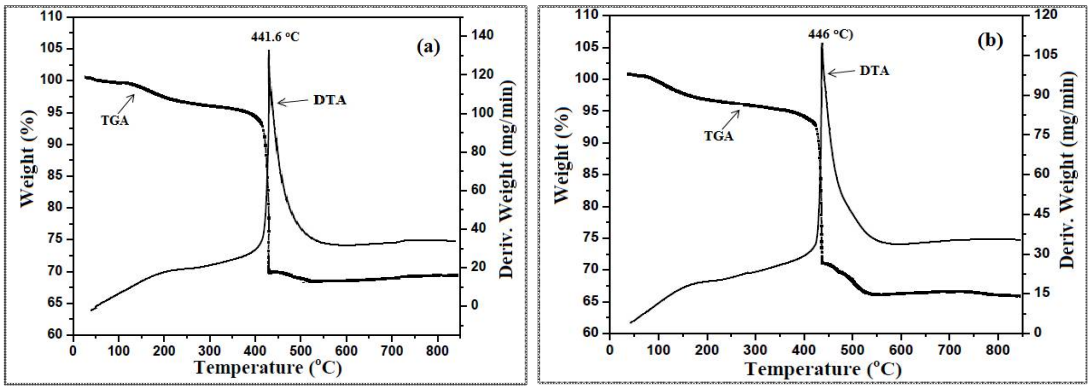

Figure 1. TGA and DTA analysis of (a) $LiNi_{0.925}Mg_{0.075}PO_4$ and (b) $LiNi_{0.9}Mg_{0.1}PO_4$ materials.

XRD analysis: The X-ray diffraction pattern of $LiNi_{0.925}Mg_{0.075}PO_4$ and $LiNi_{0.9}Mg_{0.1}PO_4$ powder samples, which are synthesized by three stapes solid state reaction method, are as shown in figure 2. Both samples show good crystallization, with sharp, strong and well defined diffraction peaks without impurities, which indicates that both samples have a single phase structure. The presence of strong

diffraction peaks with miller indices (200), (101), (210), (111), (211) (311) and (121) correspond to the formation of single phase olivine type structure of $LiNi_{0.925}Mg_{0.075}PO_4$ and $LiNi_{0.9}Mg_{0.1}PO_4$ samples, which is consistent with Joint Committee on Powder Diffraction Standards(JCPDS) file number 88-1297. This indicates that partial substitution of Mg for Ni does not change the crystal structure of $LiNiPO_4$. It is also observed that all the diffraction peaks of $LiNi_{0.925}Mg_{0.075}PO_4$ and $LiNi_{0.9}Mg_{0.1}PO_4$ are consistent with those reported earlier for pure $LiNiPO_4$ cathode.

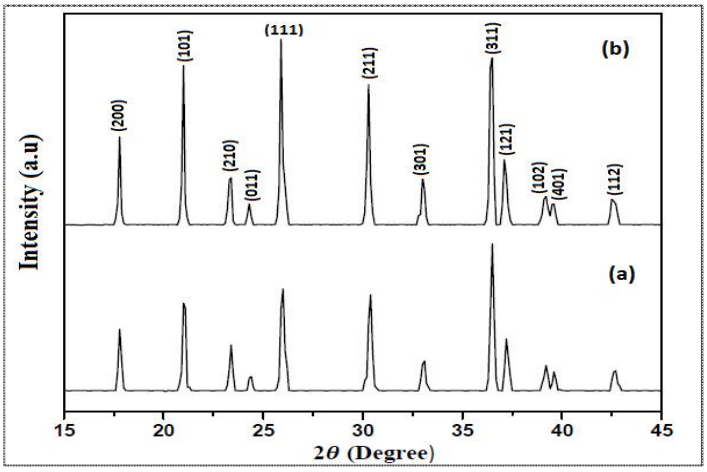

Figure 2. XRD patterns of (a) $LiNi_{0.925}Mg_{0.075}O_4$ and (b) $LiNi_{0.9}Mg_{0.1}O_4$.

From XRD patterns of both samples, it can also be observed that the intensity of the diffraction peaks increases with an increase in Mg content. This increase in intensity of the diffraction peaks is attributed to the occupancy of Mg ions which have larger ionic radii of 0.72 Å [**11, 12**]as compared to that of the Ni (0.69 Å) [**13**]. Further, the crystal sizes of both samples are calculated from (hkl) value of (111) using Scherer formula;

$$L = \frac{k\lambda}{\beta \cos\theta} \qquad (1)$$

Where L is the crystalline size, λ is the x-ray wave length, k is the shape factor of the average crystallite, β is the full width at half maximum (FWHM) in radians and θ is the diffraction angle. The crystal sizes of $LiNi_{0.925}Mg_{0.075}PO_4$ and $LiNi_{0.9}Mg_{0.1}PO_4$ are found to be 81.6 and 83.6 nm, respectively. This is associated with the larger ionic radii of Mg ions than Ni ions, as stated above. Similar results are reported by K. Anad *et al.* [**14**].

The lattice parameters as well as the corresponding unite cell volumes of both samples are calculated by using software. It is found that the lattice parameter values for $LiNi_{0.925}Mg_{0.075}PO_4$ cathode are a = 10.054 Å, b = 5.851 Å and c = 4.679 Å. Similarly, they are found to be a = 10.059 Å, b = 5.858 Å and c = 4.681 Å for $LiNi_{0.9}Mg_{0.1}PO_4$. This shows that the lattice parameters for $LiNi_{0.9}Mg_{0.1}PO_4$ slightly larger than $LiNi_{0.9}Mg_{0.1}PO_4$ sample. Moreover, the lattice parameters of the Mg^{2+}substituted synthesized samples are slightly larger when compared with the pure $LiNiPO_4$ (a = 10.03 Å, b = 5.85 Å and c = 4.69 Å) [**15**]. This effect may also be associated with the ionic radius difference between Mg and Ni cations. A similar effect is also observed in the unite cell volume, i.e. 275.246 $(Å)^3$ and 275.831 $(Å)^3$ for $LiNi_{0.925}Mg_{0.075}PO_4$ and $LiNi_{0.9}Mg_{0.1}PO_4$ cathodes, respectively. From the XRD pattern, it is also observed that a slight shift of peaks towards the left (lower 2θ angle) is observed for $LiNi_{0.9}Mg_{0.1}PO_4$ sample, indicating an increase in crystal size with an increase in Mg content. The result is consistent with the earlier observation in crystal sizes, showing the existence of a clear correlation between crystal size and the position of diffraction patterns.

EDS study: The energy dispersive spectrometer (EDS) analysis is carried out to verify the incorporation of all elements in both $LiNi_{0.925}Mg_{0.075}PO_4$ and $LiNi_{0.9}Mg_{0.1}PO_4$ samples as well as to confirm the purity of the synthesized samples. The obtained EDS spectra of both samples are shown in figure 3. As shown in the figure, Ni, Mg, P and O elements are detected in both samples which are synthesized by three steps solid state reaction methods. No other elements are detected in the samples, which indicate the purity of the prepared sample. This reviles that all the elements are incorporated in the lattice of both samples. However, lithium Li is not identified from both samples. This is due to the fact that EDS cannot detect the lightest elements, such as Li, H and He.

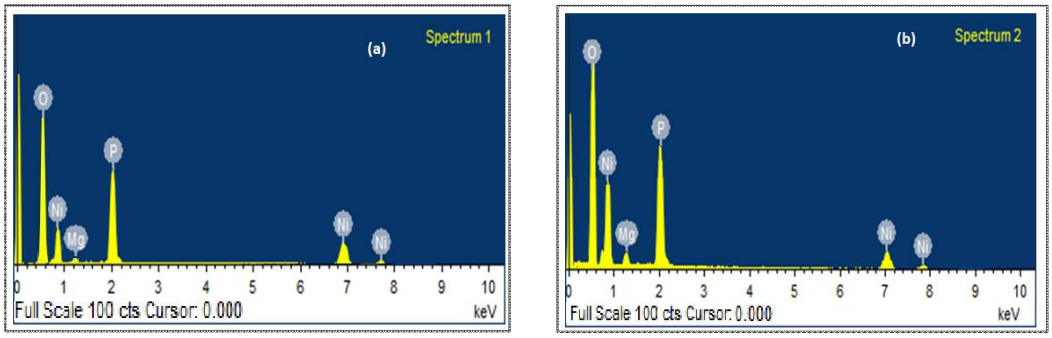

Figure 3. EDS spectra of (a) $LiNi_{0.925}Mg_{0.075}PO_4$ and (b) $LiNi_{0.9}Mg_{0.1}PO_4$ materials.

FT-IR analysis: Figure 4 shows FTIR spectra of $LiNi_{0.925}Mg_{0.075}PO_4$ and $LiNi_{0.9}Mg_{0.1}PO_4$ cathode materials prepared by three steps solid state synthesis method. It is clearly observed that these cathode materials exhibit different absorption spectral bands at different wavenumber. The band observed at 472 cm^{-1} is attributed to Li-O the intramolecular vibrations of the LiO_6 molecules. The stretching mode of MO_6 (M = Ni and Mg) distorted octahedral is observed at 647 cm^{-1}. The higher frequency vibrational band located between 961 and 1133 cm^{-1} are attributed to P-O the intramolecular vibrations of the ions in both materials. As compared the two compounds, they show similar FT-IR spectra. This result is consistent with the result obtained by K.Anad *et al.* [**14**].

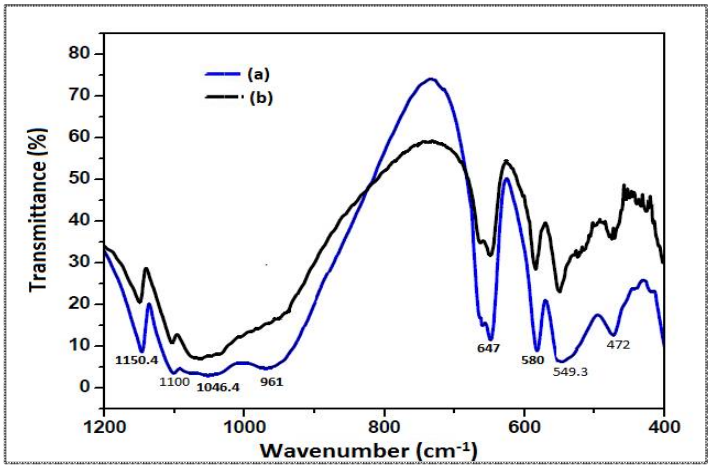

Figure 4. FT-IR spectra of (a) $LiNi_{0.925}Mg_{0.075}PO_4$ and (b) $LiNi_{0.9}Mg_{0.1}PO_4$ cathode materials.

Impedance spectroscopy study: Figure 5 show the frequency dependent of the real impedance (Z') and imaginary impedance (Z") parts of $LiNi_{0.925}Mg_{0.075}PO_4$ and $LiNi_{0.9}Mg_{0.1}PO_4$ cathode materials calculated using the relation;

$$Z' = |Z| \cos\theta \quad \text{and } Z'' = |Z| \sin\theta \qquad (2)$$

Where Z is impedance measured from the samples and θ is the phase angle. As shown from the figure 5, it is observed that the magnitude of Z′ and Z''decreases as the frequency gradually increases, indicating an increase in conductivity of both electrodes due to hopping of electrons. The decreasing values of Z′ and Z'' means that the loss in resistive property of the samples. Such a behavior is expected due to the presence of space charge polarization in both materials. Similar results have been reported by K. Vijaya Babua *et al*. [16].

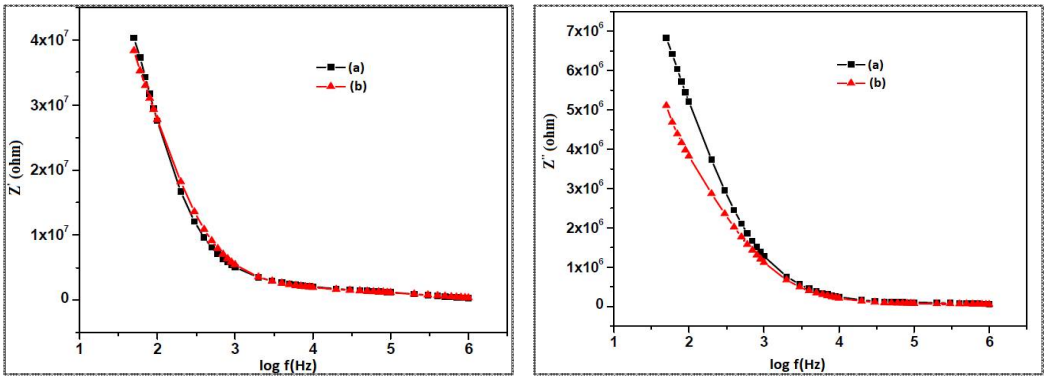

Figure 5. Frequency dependence of real impedance (***Z′***) and imaginary impedance (***Z′′***) of (a) $LiNi_{0.925}Mg_{0.075}O_4$ and (b) $LiNi_{0.9}Mg_{0.1}O_4$cathode materials.

The dielectric property of cathode materials obviously depends on the different factors, such as preparation method, types of dopants, and sintering temperature. For investigating the influence of frequency on the dielectric constant of both electrodes, the real part of dielectric constant (ε′) is calculated using the relation;

$$\varepsilon' = \frac{C\,L}{\varepsilon_o A} \qquad (3)$$

Where C is the capacitance, ε_o is the permittivity of free space, L and A are the correctional area and thickness of the pellets, respectively. The room temperature variation of ε' with respect to frequency for these electrodes coated with silver is shown in figure 6. It is observed that the dielectric constant decreases sharply at low frequency as compared to that at high frequency and become almost constant on further increasing the frequency for both samples. The higher value of ε' in the low frequency region may be due to the presence of silver electrode which is unable to permit to the transfer of mobile ions, as a result ions are accumulated near the silver electrodes and produce the bulk polarization effect in the material [17, 18]. These dielectric ions are produced may be due to the hopping between Ni^{2+} and Ni^{3+} ions. At low frequencies, the hopping frequency of charge carriers follows the applied field, which results in the increase in the dielectric constant. However, at higher frequency region, the dielectric constant ε′ begins drop and becomes constant, which is associated with the space charges not being able to follow the field variations at high frequencies. This means that at higher frequencies, the hopping frequency of charge carriers lags behind the applied field at the electrode surfaces and hence the dielectric constant decreases and becomes constant due to random dipolar orientation.

The frequency dependence ac conductivity σ_{ac} of both electrodes is calculated by using the formula;

$$\sigma_{ac} = 2\pi f \varepsilon' \varepsilon_o \tan\delta \qquad (4)$$

Where $\varepsilon_o$is the permittivity of the free spaces, f is the frequency, $\tan\delta$ is the dielectric loss tangent. The variation of the ac conductivity of both electrodes at room temperature as a function of frequency is shown in figure 6. The ac conductivity (of the synthesized materials depend on the hopping of electrons between Ni^{2+} and Ni^{3+} ions in crystal of both electrodes. As can be observed, two different regions are clearly identified in both compounds. The first one is frequency independent (dc conductivity) region, which is observed at lower frequency and the second one is the frequency

dependent (ac conductivity) region observed at higher frequencies. The increasing of ac electrical conductivity in high frequency region can be related to the electronic polarization as well as to the hopping of charge carrier over a small barrier height. However, the dc conductivity at low frequency side due to long range migration of charge carriers, which is a normal behavior of $LiNiPO_4$ based cathode materials [**14, 16**].

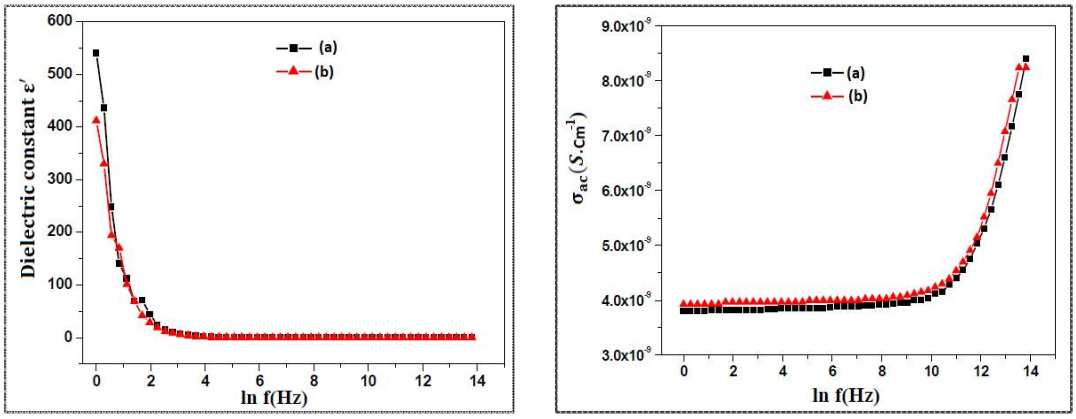

Figure 6. Frequency dependencies of dielectric constant ($\boldsymbol{\varepsilon'}$) and ac conductivity ($\boldsymbol{\sigma_{ac}}$) for (a) $LiNi_{0.925}Mg_{0.075}O_4$ and (b) $LiNi_{0.9}Mg_{0.1}O_4$materials.

The dc conductivity values of both cathode materials are calculated using the equation;

$$\sigma_{dc} = \frac{L}{R_b A} \qquad (5)$$

Where L is the thickness of the pellet R_b is the bulk (grain) resistance and A is the correctional area of the pellets. It is found that the dc conductivities of $LiNi_{0.925}Mg_{0.075}PO_4$ and $LiNi_{0.9}Mg_{0.1}PO_4$ compounds are 3.8 x 10^{-9} and 3.94 x 10^{-9} S cm^{-1}, respectively. K. Anand *et. al.*, [**14**] has reported that the dc conductivity of $LiNiPO_4$ cathode material at room temperature is in the order of 10^{-10} S cm^{-1}. We feel that the results obtained for the investigated samples are compatible. Also, the obtained conductivity results are found in the range of the electrical conductivity of semiconductor (10^{-7} to 10^{3} S cm^{-1}), indicating the semiconductor behavior of the samples.

APPLICATION

The main applications of oliven structured cathode materials are in electrochemical in electrical energy storage systems. Therefore, $LiNi_{0.925}Mg_{0.075}PO_4$ and $LiNi_{0.9}Mg_{0.1}PO_4$ materials can be used as cathode materials in lithium ion battery technology.

CONCLUSIONS

The present research work reveals the successful synthesis of Mg substituted $LiNiPO_4$ cathode materials by three steps solid state synthesis method. From the thermal property study, the weight loss regions are identified up to 550^0C due to the decomposition of the precursors. The XRD technique identifies the single phase formation of $LiNi_{0.925}Mg_{0.075}PO_4$ and $LiNi_{0.9}Mg_{0.1}PO_4$, indicating the successful synthesis of both materials. From the EDS spectra, all components of the synthesized samples are identified. No other elements are recognized, which is consistent with the result obtained in the XRD patterns. From room temperature measurement of dielectric constant, it is found that the dielectric constant decreases sharply at low frequency as compared to that at high frequency and become almost constant on further increasing the frequency for both samples. The room temperature

electrical conductivity of $LiNi_{0.925}Mg_{0.075}PO_4$ and $LiNi_{0.9}Mg_{0.1}PO_4$ are found to be 3.8 x 10^{-9} and 3.94 x 10^{-9} S cm^{-1}, respectively.

REFERENCES

[1]. B. Xu, D. Qian, Z. Wang, Y. S. Meng, *Mat Sci &Eng R*, **2012**, 73, 51–65.
[2]. S. M. Rommel, N. Schall, C. Brunig, R. Weihric, *Monatsh Chem*, **2014**, 40, 145-385.
[3]. R. Qing, M. C. Yang, Y. S. Meng, W. Sigmund, *Electrochim Acta*, **2013**,108, 827-832.
[4]. M. Sathiya, Annigere, S. Prakash, K.Ramesha, A. K. Shukla, *Mater*, **2009**, 2, 857-868.
[5]. Y. Bai, P. Qiu, Z. Wen, S, Han, *J Alloys & Compd*, **2010**, 508, 1-4.
[6]. *O. Toprakci, H. A. K. Toprakci*, L. Ji, *X, Zhang, Kona Powder Part J, **2010**, 28,* 50–73.
[7]. H. Aono, E. Sugimoto, Y. Sadaoka, N. Imanaka , G. Adachi, *Solid State Ion, **1990**, 40/4*, 38-42.
[8]. I. Abrahams, E. Hadzifejzovic, *Solid State Ion*, **2000**,134, 249-257.
[9]. S. Tobishima, K. Takei, Y. Sakurai, J. Yamaki, *J Power Sources*, **2000**, 90, 188-195.
[10]. M. Yang, J. Hou, *Membranes*, **2012**, 2, 367-383.
[11]. H. Nur, H. Hamdan, *Mater Res Bull*, **2001**, 36,315-322.
[12]. M. V. Reddy, T. W. Jie, C. J. Jafta, K. I. Ozoemena, M. K. Mathe, A. S. Nair, S. S. Peng, M. S. G. Idris Balakrishna, F. I. Ezema, B. V. R. Chowdari, *Electrochim Acta*, **2014**,128 192–197.
[13]. R Qing, M. C. Yang, Y. S. Meng, W. Sigmund, *J Electrochim Acta*, **2013**,108, 827-832.
[14]. K. Anand, B. Ramamurthy, V. Veeraiah, K. V. Babu, *J Mater Sci-Poland*, **2017**, 35, 66-80.
[15]. Gangulibabu, D. Bhuvaneswari, N. Kalaiselvi, N. Jayaprakash, P. Periasamy, *J Sol-Gel Sci Technol*, **2009**, 49,137-144.
[16]. K. V. Babu, L. S .Devi, V. Veeraiah, K. Anand, *J.Asian Ceram Soc*, **2016,** 4, 269-276.
[17]. A. Dutta, T.P. Sinha, P. Jena, S. Adak, *J Non-Cryst* Solids, **2008,** 354, 3952-3957.
[18]. D. K. Mahato, A. Dutta, T .P. Sinha, *Phys B*, **2011**, 406, 2703.